Disorder correction to equilibrium in a perfect electric wire

Eric Bringuier[1*]
[1] Matériaux et Phénomènes Quantiques, Unité mixte 7162 CNRS & Université de Paris Cité, case 7021, 5 rue Thomas Mann, 75205 Paris Cedex 13, France

Abstract. Quantum coherence properties are attractive for making a quantum computer, but they are easily destroyed by environmental disorder. This contribution examines a way of achieving a perfect electric wire of gallium arsenide such that charge carriers move unscattered despite the environmental disorder due to the unavoidable thermal agitation. The example is academic yet experimental. Carrier motion through the crystal is theoretically investigated within a fully quantum framework, simpler than decoherence theory, where the occupancy of classical states is replaced by a Wigner function. The effect of a weak disorder is accounted for analytically by means of a multiple-scale method without a Markov assumption. Even though carriers do move ballistically over several micrometres, the thermal disorder gives rise to important fluctuations about the thermodynamic equilibrium state at temperatures above 0.05 K.

1 By way of introduction: the ongoing search for a quantum computer

A quantum computer is expected to make use of uniquely quantum features, such as superposition states endowed with interference capability, in order to tackle some problems at a much higher speed than a computer based on classical binary digits. In 2000 a quantum computer was deemed to be within reach according to IBM and MIT experts [1]. In 2024, however, the advent of a quantum computer or more likely add-ons to conventional machines—coprocessors performing specific tasks in the same way that a graphics card takes over the most difficult display chores—remains elusive [2]. Several technologies are envisaged for a quantum computer; herein we shall be interested in an issue relevant to the putative circuitry of a solid-state electron-based computer. A key problem is that the quantum-coherence features of the system of interest—here, a conduction electron in a crystalline solid—quickly get lost owing to interaction with the environment—here, the lattice of atoms. In decoherence theory [3], the degrees of freedom of the system are entangled with the many ones of the environment. Averaging over the environmental degrees of freedom tends to suppress coherences, i.e. off-diagonal terms, of the statistical matrix of the system in a certain basis. This turns a coherent superposition into an incoherent mixture in the chosen basis. Although decoherence theory has been confirmed by experiment, it quickly becomes intractable when dealing with solid-state issues. Now an alternative, simpler viewpoint to decoherence theory, rooted in the analogy of matter and light waves, has been developed in previous works [4, 5]. Despite the difference in the wave equations of d'Alembert and Schrödinger, the Verdet–Rayleigh theorem of scalar optics —the superposition of amplitudes ending up in the addition of light intensities [6, 7]— has a counterpart in matter waves. Fluctuations in the potential energy sensed by an electron moving in a solid are similar to fluctuations in the optical refraction index blurring out the coherence of a light beam [8]. Our goal in this paper is to make use of this simpler framework to theoretically investigate the behaviour of a 'perfect' [9] solid electric wire in which a conduction electron does not collide with the lattice of atoms over the length of the wire. An electron which has a negligibly low probability of colliding with the lattice has its wave-mechanical coherence preserved during transport along the wire. To be physically realistic, we shall consider a wire that has been experimentally implemented in a real device [10–12]. The example is somewhat academic, but it is not a *Gedankenexperiment*.

The layout of the paper is as follows. Section 2 describes an experimental electric wire where electrons move almost unscattered over a significant distance so that quantum coherence is preserved. The physical parameters of this particular system are extracted from experiment so as to provide a quantitative basis for a later analysis. Next, sections 3–5 epitomize the quantum theory of electron transport used in this paper to supersede the semiclassical framework of Bloch and Sommerfeld as reviewed by Bardeen [13]. Sections 3–5

* Corresponding author : eric.bringuier@univ-paris-diderot.fr

are intended to introduce the theoretical tools and notations and make the paper self-contained. They may be skipped by readers aware of previous papers [4, 5, 14] based upon an approach developed in vacuum by Henkel [15] after [16]. Specifically, in section 3 Schrödinger's account of electron dynamics in a crystal is replaced by Wigner's which is akin to classical statistical physics in phase space [17]. Section 4 sketches the transformation of Wigner's reversible dynamical equation into an irreversible transport equation due to disorder. No Markov assumption is needed. The disorder considered in later sections is the thermal agitation of the lattice hosting mobile electrons. Section 5 includes the changes needed to account for the fermionic nature of electrons and the bosonic nature of the quantized lattice waves involved in the microphysics of thermal agitation. Section 6 specializes the theory of sections 3–5 to the thermodynamic equilibrium state. The correction to the equilibrium occupancy due to the thermal disorder is examined. This correction is calculated in section 7 with parameters taken from the experimental electron gas of section 2. Conclusions are drawn in section 8.

2 An example of a perfect electric wire

This section describes an experimental example of an almost perfect electric wire whose characteristic physical quantities will be used in section 7. In the 1980s, quasi-two-dimensional (2D) electron gases have been achieved in highly crystalline, very pure GaAs at the interface with AlGaAs, as shown in Fig. 1a.

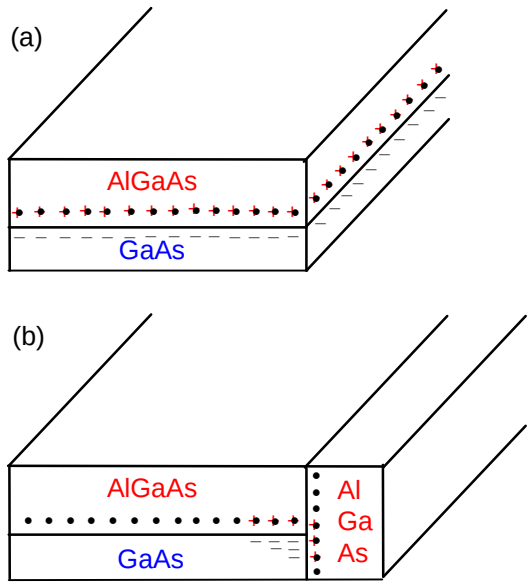

Fig. 1. (a) Ionisation of donor impurities (shown as dots) lying in an AlGaAs layer gives rise to a quasi-2D electron gas in the undoped GaAs layer beneath. (b) Another doped AlGaAs layer is overgrown on one edge of the AlGaAs–GaAs structure. Attraction by the ionised impurities of the two AlGaAs layers confines the electron gas in a wedge of the GaAs layer.

Once donor (Si) impurities located in AlGaAs ionize, their electrons go to states of lower energy available in the GaAs conduction band whose bottom lies below that of AlGaAs. The electrons stay near the interface because of attraction by the positively ionized donors; there is an abundant literature on such 'quantum wells' [18]. In the structure of Pfeiffer *et al.* [10, 11], a new doped AlGaAs layer is epitaxially overgrown on one edge of the GaAs–AlGaAs heterostructure; see Fig. 1b. Upon ionisation of the new dopants, the GaAs electron gas is attracted in a wedge of the GaAs layer. Charge transport is then possible only within a pipe.

In [11] an electron gas of number density $n_{2D} \approx 2.5\text{x}10^{15}$ m^{-2} has been achieved in GaAs. Given the quasi-2D density of states per unit energy $dn_{2D}/dE = m^*/\pi\hbar^2$ [18], where $m^* = 0.067\,m_0$ is the effective mass and m_0 is the free electron mass, conduction states are occupied up to energy level $E_c + E_F$, where E_c is the GaAs conduction-band bottom, and

$$E_F = \left(\frac{\pi\hbar^2}{m^*}\right) n_{2D} = 8.9\text{x}10^{-3}\ \text{eV}. \qquad (1)$$

The border between occupied and empty states is sharp at temperature $T = 4$ K because $kT = 3.5\text{x}10^{-4}$ eV is much less than E_F, as shown in Fig. 2.

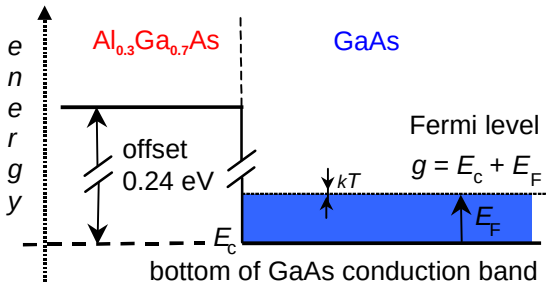

Fig. 2. The energy scales in the GaAs quasi-2D electron gas of [11]: $Al_{0.3}Ga_{0.7}As$–GaAs conduction-band offset, Fermi energy $E_F = 8.9\text{x}10^{-3}$ eV, and typical thermal energy $kT = 3.5\text{x}10^{-4}$ eV. The typical electron-phonon energy interchange, $m^*c_s^2 = 5.6\text{x}10^{-6}$ eV, is not shown. Energy as reckoned along the vertical axis does not include the potential energy of the macroscopic electric field caused by the distribution of free charge.

In GaAs we have a degenerate gas of chemical potential $g = E_c + E_F$, also called the Fermi level. Electrons lying near this level have a random velocity of given modulus $v_F = (2E_F/m^*)^{1/2} = 2.2\text{x}10^5$ m/s. They respond to an electrochemical gradient $\nabla\tilde{g}$, where $\tilde{g} \equiv g + \bar{e}V$ includes the electrostatic potential energy $\bar{e}V$ and $\bar{e} \equiv -e$ is the signed electron charge, with a drift velocity $\mu\nabla(-\tilde{g})$, and $e\mu$ is the drift mobility. Its value is measured to be very large, $e\mu = 4\text{x}10^6$ cm^2 V^{-1} s^{-1}, at 0.3 K This, according to Drude's formula, points to a very long velocity-relaxation time, $\tau_v = m^*\mu = 1.5\text{x}10^{-10}$ s. The associated mean free path (mean distance travelled forward before the initial motion is randomized) at 0.3 K,

$$\lambda = v_F\tau_v = 33\ \mu\text{m}, \qquad (2)$$

is large. The probability of a given electron maintaining its initial motion after crossing a distance L is $\exp(-L/\lambda)$. If this probability can be neglected, one speaks of ballistic transport.

The microscopic explanation for the large mean free path is that mobile electrons in GaAs cannot be scattered by ionized donors which lie in AlGaAs. The only scattering mechanism is with lattice vibrations unless residual unintentional impurities are present [19]. Scattering with optical vibrations is excluded because

(i) absorption of optical phonons is negligible as their population at 4 K is negligible;

(ii) emission of optical phonons is negligible, too, as their energy largely exceeds kT, which is the typical energy difference between initial and final electron states in an electron-phonon scattering event.

Therefore, conduction electrons are scattered only by acoustic vibrations. The typical energy interchange in a scattering event is $\pm m^* c_s^2$, where $c_s = 4.0\times10^3$ m/s is the speed of sound; this value is an average over polarizations and directions of acoustic waves [20]. Because $m^* c_s^2 = 5.6\times10^{-6}$ eV is much less than kT, electron-phonon scattering is almost elastic, i.e. it almost conserves the electron's energy. The mean phonon occupation number $\langle n_{\mathbf{q}} \rangle$ is related to the phonon energy $\hbar\omega_{\mathbf{q}}$ through the Bose–Planck formula,

$$\langle n_{\mathbf{q}} \rangle = \frac{1}{\exp(\hbar\omega_{\mathbf{q}}/kT) - 1} \approx \frac{kT}{m^* c_s^2} = 62. \qquad (3)$$

This number is large, $\langle n_{\mathbf{q}} \rangle + 1 \approx \langle n_{\mathbf{q}} \rangle$, and classical equipartition statistics is relevant.

In [10, 11] a lateral doped AlGaAs layer is overgrown, the ionized donors of which attract the electron gas on one side of the GaAs layer. This turns the layer of mobile electrons in Fig. 1a into a wire in Fig. 1b. In the authors' words, 'the resultant wire resides all along an atomically precise edge of a GaAs quantum well'. The probability of ballistic transport over a wire length L = 6 µm is $\exp(-6/33) = 83\,\%$. Besides the scarcity of scattering events, the typical energy interchange upon scattering with an acoustic phonon is $m^* c_s^2 \ll kT \ll E_F$. The upshot is that the wire is expected to have negligible electrical resistance. In the experiment, a small voltage U applied across entry (source) and exit (drain) of the wire, not shown in Fig. 1, was observed to cause an electric current $I \propto U$. The conductance $G \equiv U/I$ showed discrete steps depending on the voltage of auxiliary gate electrodes, shown in Fig. 1 of [11]. This phenomenon of conductance quantization is related to the transverse confinement of matter waves [21–23]. The resistanceless nature of the ballistic wire *itself*, excluding the entry and exit terminals across which U is measured, was checked by means of a four-terminal measurement device; no voltage was measured across two probes located along the wire; that is, the profile of electrochemical potential is flat within the wire while current is flowing therein [11, 24].

To conclude this section, such a wire is an —admittedly academic— potential candidate for use in an electron-based quantum computer, notwithstanding practical implementation problems. The goal of this paper is to work out a quantum theory of electron transport in an electron gas going beyond the semi-quantum description of Bloch and Sommerfeld [13]. Because we are interested in conceptual and semi-quantitative aspects, we shall not consider a realistic geometry of the wire, which would require a numerical treatment. Instead, we shall consider a three-dimensional (3D) electron gas with the same values of E_F and v_F. Since $E_F = \hbar^2(3\pi^2 n_{3D})^{2/3}/2m^*$ in a 3D gas of electron density n_{3D}, this means a typical inter-electron distance $n_{3D}^{-1/3} = 25$ nm in our 3D calculations in section 7 instead of $n_{2D}^{-1/2} = 20$ nm in the experimental system.

3 Electron motion: from Schrödinger's quantum dynamics to Wigner's

For the sake of self-containedness, this section and the two following ones sketch the theoretical framework used, which is justified at length in [4, 14] based on [15, 16]. We start from the one-electron state vector which obeys Schrödinger's dynamical equation including all interactions sensed by the electron. The state vector is a wave function $\psi(\mathbf{r}, t)$ whose dynamics is governed by

$$\frac{\partial\psi}{\partial t} = \frac{1}{\mathrm{i}\hbar}\Big[\frac{1}{2m_0}(-\mathrm{i}\hbar\nabla)^2 + U_0(\mathbf{r}) + U_1(\mathbf{r}) + U_2(\mathbf{r})\Big]\psi. \quad (4)$$

Three potential energies are involved in (4): $U_0(\mathbf{r})$ is the periodic crystal potential, $U_1(\mathbf{r})$ is the applied electrostatic potential energy $\bar{e}V(\mathbf{r})$, and lastly $U_2(\mathbf{r})$ is either a static disordered energyscape due to defects and impurities [4] or a time-dependent energyscape $U_2(\mathbf{r}, t)$ due to the thermal agitation of the lattice, which consists of a random superposition of elastic waves of all wave-vectors [14]. The dynamical equation (4) is subsequently transformed within a chain of controllable approximations which are merely sketched out here.

In a first step, the dominant interaction $U_0(\mathbf{r})$ is handled by replacing the waveform ψ by its envelope $\tilde{\psi}$ whose dynamics is governed by a Schrödinger-like equation,

$$\frac{\partial\tilde{\psi}}{\partial t} = \frac{1}{\mathrm{i}\hbar}\Big[E(-\mathrm{i}\hbar\nabla) + U_1(\mathbf{r}) + U_2(\mathbf{r})\Big]\tilde{\psi}, \qquad (5)$$

where $E(\mathbf{p})$ is the dispersion relation of a Bloch wave in the array of atoms, and the pseudomomentum $\mathbf{p}$ is $\hbar$ times a pseudo-wave-vector lying in the fundamental Brillouin zone (BZ) of the crystal. This is a continuum description where local atomicity is smoothed out. Fine-scale features may be included through a systematic expansion in powers of the lattice spacing [25].

In a second step, one defines the real-valued Wigner transform f_W of the complex-valued effective wave function $\tilde{\psi}$,

$$f_W(\mathbf{r}, \mathbf{p}) = \int_\Omega \tilde{\psi}\Big(\mathbf{r}+\frac{\mathbf{s}}{2}\Big)\,\tilde{\psi}^*\Big(\mathbf{r}-\frac{\mathbf{s}}{2}\Big)\exp\Big(-\frac{\mathrm{i}\mathbf{p}\cdot\mathbf{s}}{\hbar}\Big)\,\mathrm{d}^3\mathbf{s}, \qquad (6)$$

where Ω is the crystal volume, and the time dependence is omitted for a simpler notation. An equivalent definition exists in terms of the spatial Fourier transform, defined on the BZ, of $\tilde{\psi}$ [4]. For a normalized wave function, we have

$$\int_{\Omega}\int_{\mathrm{BZ}} f_{\mathrm{W}}(\mathbf{r},\mathbf{p})\frac{\mathrm{d}^3\mathbf{r}\,\mathrm{d}^3\mathbf{p}}{h^3}=1. \qquad (7)$$

The rationale for the Wigner function f_{W} is that it enables one to calculate the expectation value of any function $F(\mathbf{r}) + G(\mathbf{p})$ in the way of classical statistical physics [17], namely

$$\overline{F(\mathbf{r})+G(\mathbf{p})}=\int_{\Omega}\int_{\mathrm{BZ}}\left[F(\mathbf{r})+G(\mathbf{p})\right]f_{\mathrm{W}}(\mathbf{r},\mathbf{p})\frac{\mathrm{d}^3\mathbf{r}\,\mathrm{d}^3\mathbf{p}}{h^3}. \qquad (8)$$

A Wigner function may, however, take *negative* values; it is a *quasi*-probability function which reflects the *non-classical* nature of the dynamics.

For slowly-varying functions $E(\mathbf{p})$ and $U_1(\mathbf{r})$, the evolution of f_{W} is governed by [4]

$$\frac{\partial f_{\mathrm{W}}}{\partial t}\approx-\left(\frac{\partial E}{\partial \mathbf{p}}\right).\frac{\partial f_{\mathrm{W}}}{\partial \mathbf{r}}-\left(\frac{\partial U_1}{\partial \mathbf{r}}\right).\frac{\partial f_{\mathrm{W}}}{\partial \mathbf{p}}$$
$$+\frac{\mathrm{i}}{\hbar}\int_{\mathrm{BZ}}\frac{\Omega\,\mathrm{d}^3\mathbf{q}}{(2\pi)^3}\hat{U}_2(\mathbf{q})\times$$
$$\left[f_{\mathrm{W}}\left(\mathbf{r},\mathbf{p}+\hbar\frac{\mathbf{q}}{2}\right)-f_{\mathrm{W}}\left(\mathbf{r},\mathbf{p}-\hbar\frac{\mathbf{q}}{2}\right)\right]\mathrm{e}^{\mathrm{i}\mathbf{q}.\mathbf{r}}, \qquad (9)$$

where $\hat{U}_2$ denotes the spatial Fourier transform of U_2. This Wigner dynamical equation is formally similar to the Liouville equation governing the phase-space distribution function in classical statistical physics, with a difference. While the effect of the slowly-varying U_1 is embodied in a Liouville-like differential term, the effect of U_2 is embodied in an integral term; large $\mathbf{q}$ values in the spatial Fourier transform $\hat{U}_2$ are involved insofar as U_2 varies over small $\mathbf{r}$ scales. In this work U_2 will stand for the electron-lattice interaction energy, and the thermally agitated lattice is the seat of a superposition of random elastic waves.

A transport problem is not concerned with one particle moving in a given volume Ω. Often one has to do with several electrons of given chemical potential. The electron number N is well-defined on the average, but it may take values around the average. One defines an N-particle Wigner function $f_{\mathrm{W}}^{(N)}$ which obeys an N-particle dynamical equation. From $f_{\mathrm{W}}^{(N)}$ a reduced 1-particle Wigner function $f_{\mathrm{W}}^{(1)}$ is defined such that [26, 27]

$$\int_{\mathrm{BZ}} f_{\mathrm{W}}^{(1)}(\mathbf{r},\mathbf{p})\frac{\mathrm{d}^3\mathbf{p}}{h^3}=n(\mathbf{r}) \qquad (10)$$

is the particle density at location $\mathbf{r}$. The function $f_{\mathrm{W}}^{(1)}$ is not normalized as its integral over phase space is N. The Wigner dynamical equation governing function $f_{\mathrm{W}}^{(1)}$ is again (9) if interaction between particles is neglected. In the following f_{W} will stand for the reduced 1-particle function $f_{\mathrm{W}}^{(1)}$.

So far we have been considering the dynamics of *one* particle. Transport, however, is inherently statistical so that only the mean values of quantities are to be considered. This was already so in classical physics. Quotation from Maxwell [28]: 'everything depends on these mean values. [...] I carefully abstain from asking the [particles] where they last started from. I only count them and register their mean velocities, avoiding all personal enquiries' of particles. The following section proceeds from a *mechanical* description of individuals to a *statistical*-mechanical one of a collective of particles. Thus, irreversibility arises from releasing information.

4 From reversible motion to irreversible transport

This section sketches how the disordered potential energy U_2 affects the Wigner dynamics of conduction electrons. Whether static or time-dependent, a disordered potential is a stochastic scalar field which has a multiplicity of realisations. Such a field is defined statistically via its first, second, third... moments,

$$\langle U_2(\mathbf{r})\rangle,\quad \langle U_2(\mathbf{r}+\mathbf{s})U_2(\mathbf{r})\rangle,$$
$$\langle U_2(\mathbf{r}+\mathbf{s}')U_2(\mathbf{r}+\mathbf{s})U_2(\mathbf{r})\rangle,$$
$$\ldots \qquad (11)$$

where $\langle..\rangle$ denotes the averaging over the ensemble of realisations. We shall consider a statistically homogeneous field, the moments of which do not depend on $\mathbf{r}$, that is to say

first moment $\langle U_2(\mathbf{r})\rangle = \langle U_2\rangle$ (mean),
centred second moment
$$\left\langle[U_2(\mathbf{r}+\mathbf{s})-\langle U_2\rangle][(U_2(\mathbf{r})-\langle U_2\rangle]\right\rangle$$
$$\equiv C_U(\mathbf{s}) \quad \text{(covariance)},$$
$$\ldots \qquad (12)$$

The characteristic length l_{c} of the covariance function C_U is called the correlation length of the disordered energyscape. In the case of a time-dependent U_2 we shall consider that the field is statistically stationary, i.e. its moments do not depend on t either. This is obviously true for thermal agitation of the lattice at a given temperature.

This connection between disorder and multiplicity is the one of statistical physics as illustrated on the example of the tossing of $\mathcal{N}$ coins. Quotation from [29]: 'If $\mathcal{N}$ pennies are laid out on a table with all heads up [...] and $\mathcal{N}$ is large, it is highly unlikely that such an arrangement would be achieved by random tosses of the coins. For some reason, the pennies must have been deliberately laid out that way; that is, the array is ordered. [The multiplicity] $\mathcal{W}= 1$ for this arrangement. If the number of heads in any arbitrarily chosen region of the array is close to the number of tails, one would say that the array is disordered, and the arrangement could well be the result of random tosses. This arrangement [...] has a large multiplicity: $\mathcal{W} \sim 2^{\mathcal{N}}$. [...] In general we can say that *small multiplicity implies order*, while *large multiplicity implies disorder* in the sense that an arrangement with large $\mathcal{W}$ could be achieved by a random process, while one with small $\mathcal{W}$ is very unlikely to be'. This example is tantamount to a large set of spins on a lattice in the physics of magnetism. Because the natural logarithm of multiplicity $\mathcal{W}$ is the entropy reckoned in units of the Boltzmann constant k in the limit $\mathcal{N} \gg 1$, entropy is often viewed as an evaluation of disorder.

If disorder is strong, a travelling matter wave cannot exist. Whatever the wave vector, the randomness of the energyscape prevents constructive interference of scattered wavelets so that any eigenfunction of the Schrödinger equation is localized [30]. This case is excluded in this paper. We address the opposite case of a weak disorder such that the deterministic periodic U_0 dominates the random U_2, i.e. $|\nabla U_0| \gg |\nabla U_2|$. Now a

random U_2 entails a random ψ or f_W. For a weak disorder it is expected that a realisation of f_W hardly departs from the mean $\langle f_W\rangle$. Specifically, the weak fluctuation about the mean, $f_W - \langle f_W\rangle$, will scale like the root-mean-square deviation, namely $u_0 \equiv \sqrt{C_U(\mathbf{s}=0)}$. This is shown in Fig. 3 below.

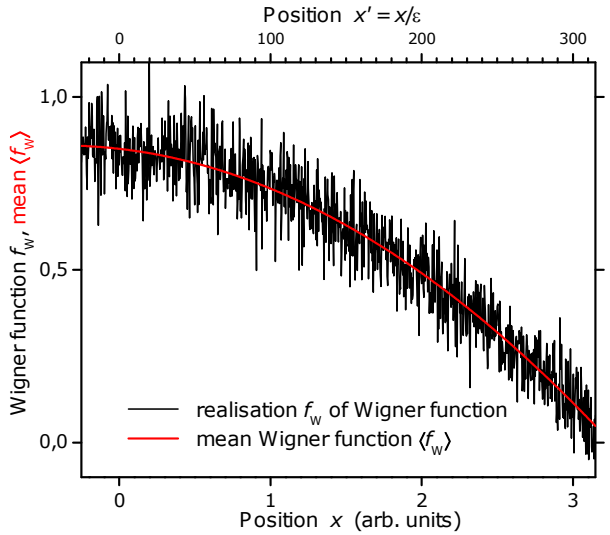

Fig. 3. Typical Wigner function $f_W(x, p, t)$ at given p and t in one dimension x. The function f_W varies over two space scales, macro- and microscopic. The latter is the correlation length of the disordered energyscape. The mean function $\langle f_W\rangle$ over all realisations of the disorder, whether static or time-dependent, varies on the macroscopic scale only.

Let us attempt a perturbation expansion in powers of a small dimensionless disorder parameter $\eta \propto u_0$,

$$f_W = f_0 + \eta f_1 + \eta^2 f_2 + O(\eta^3), \qquad (13)$$

where the main contribution f_0 is the deterministic function $\langle f_W\rangle$ while the corrections f_1, f_2 ... are stochastic of zero mean; and we seek for a closed evolution equation bearing on f_0 alone. This is achieved if the expansion (13) is traded for a multiple-scale expansion taking advantage of the disparate length scales involved [4, 15, 16, 31, 32]. In Fig. 3 a formally independent position variable, $\mathbf{r'} \equiv \mathbf{r}/\varepsilon$ with $\varepsilon \ll 1$, is added; while $\mathbf{r'}$ changes by one correlation length, $\mathbf{r}$ changes by a small amount εl_c. While U_2 is a function of the 'fast' variable $\mathbf{r'}$, in contrast U_1 is a function of the 'slow' position variable $\mathbf{r}$. Next, one takes advantage of the ergodicity of the random field f_W: 'a random field is ergodic if all information about its statistics can be obtained from a single realisation of the field' [33]; see also [34]. For an ergodic random field of correlation length l_c, the *ensemble* average $\langle..\rangle$ is identical with a *space* average over a volume l_c^3 or more. This is relevant for a macroscopic volume $\Omega \gg l_c^3$. By construction, f_0 only depends on the slow variable $\mathbf{r}$ —at given $\mathbf{p}$ and t— whereas f_1 also depends on the fast variable $\mathbf{r'}$ —at given $\mathbf{p}$ and t— and likewise for f_2. It turns out that the appropriate choice of ε is η^2, that is to say f_W is expanded in powers of $\varepsilon^{1/2}$ [4, 5, 15, 16]. Then, the closed-form kinetic equation on f_0 derived from (9),

$$\frac{\partial f_0}{\partial t} + \left(\frac{\partial E}{\partial \mathbf{p}}\right)\cdot\frac{\partial f_0}{\partial \mathbf{r}} + \left(-\frac{\partial U_1}{\partial \mathbf{r}}\right)\cdot\frac{\partial f_0}{\partial \mathbf{p}} = \int_{BZ} \frac{d^3\mathbf{p'}}{h^3}\left[W_{\mathbf{p'},\mathbf{p}} f_0(\mathbf{r},\mathbf{p'},t) - W_{\mathbf{p},\mathbf{p'}} f_0(\mathbf{r},\mathbf{p},t)\right], \qquad (14)$$

is of the linear Boltzmann type. The right-hand side exhibits a gain-minus-loss pattern which makes it interpretable as a classical scattering integral. This kinetic equation subsumes quantum features:

(i) the classical velocity in vacuum $\mathbf{p}/m_0$ is replaced by Bloch's *group velocity* $\partial E/\partial \mathbf{p}$, with $\mathbf{p}$ being restricted to the Brillouin zone; as a result, the free-electron mass m_0 is replaced by a much lighter effective mass m^* in GaAs near the conduction-band bottom;

(ii) the classical scattering cross section by potential U_2 in $W_{\mathbf{p'},\mathbf{p}}$ is replaced by the *quantum* cross section —in the first Born approximation— which often is quite different.

Two more remarks are in order:

(iii) the time-reversal symmetry of equation (9) governing f_W is broken in equation (14) governing the evolution of the mean function $f_0 = \langle f_W\rangle$;

(iv) the multiple-scale method provides the first stochastic correction f_1 to f_0; for $f_0(\mathbf{r}, \mathbf{p})$ of 'isotropic' pattern $f_e(\mathbf{r}, E(\mathbf{p}))$, the correction [4]

$$f_1(\mathbf{r},\mathbf{r'},\mathbf{p},t) = \left(\frac{\partial f_e}{\partial E}\right)_{\mathbf{r}} u(\mathbf{r'},t) \qquad (15)$$

is proportional to the fluctuation in the potential energy, namely $u(\mathbf{r'},t) \equiv U_2(\mathbf{r'},t) - \langle U_2\rangle$.

In the scattering integral, the transition rate from a state $\mathbf{p}$ to $\mathbf{p'}$ is given exactly by the golden rule with no energy broadening. This removes a long-standing problem in the derivation of a rate (master) equation from the Schrödinger dynamical equation [35, 36]. Two cases arise according as the energyscape is static or time-dependent, as displayed in Table 1. Also we note that no Markov property of the dynamics has been invoked in deriving the kinetic equation (14).

Table 1. The energy dependence of the transition rate in the Boltzmann equation is related to the time dependence of the disordered potential. The second line refers to a time-harmonic $U_2(\mathbf{r'},t) \propto \mathrm{Re}\{A_{\mathbf{q}}\exp[\pm i(\mathbf{q}\cdot\mathbf{r'} - i\omega_{\mathbf{q}}t)]\}$.

Static $U_2(\mathbf{r'})$	$W_{\mathbf{p},\mathbf{p'}} \propto \delta(E(\mathbf{p'}) - E(\mathbf{p}))$	elastic scattering
Time-harmonic $U_2(\mathbf{r'},t)$	$W_{\mathbf{p},\mathbf{p'}} \propto \delta(E(\mathbf{p'}) - E(\mathbf{p}) \pm \hbar\omega_{\mathbf{q}})$	inelastic scattering

5 Inclusion of quantum statistics

So far we have accounted for *quantum-dynamical* features while ignoring *quantum-statistical* features. Now electrons are fermions exhibiting Pauli exclusion, while elastic plane waves $U_2(\mathbf{r},t) \propto \mathrm{Re}\{A_{\mathbf{q}}\exp[\pm i(\mathbf{q}\cdot\mathbf{r} - \omega_{\mathbf{q}}t)]\}$ are quantized as bosons. These statistical features

are included by means of a procedure known as second quantization:

(i) the scalar field ψ is replaced by an operator field Ψ obeying an anti-commutation relation [37]; this gives rise to exclusion factors in the scattering term of the kinetic equation,

$$\int_{\mathrm{BZ}} \frac{\mathrm{d}^3\mathbf{p}'}{h^3} \{W_{\mathbf{p}',\mathbf{p}} f_0(\mathbf{p}')[1-f_0(\mathbf{p})] - W_{\mathbf{p},\mathbf{p}'} f_0(\mathbf{p})[1-f_0(\mathbf{p}')]\}, \tag{16}$$

just as in the semiclassical kinetic theory [13, 38] (time and position dependencies have been omitted in (16) to alleviate the notation);

(ii) a scalar field U_2 entails identical rates of absorption and emission processes for a given mode $\mathbf{q}$, just as happens when a two-level atom interacts with an electromagnetic plane wave in vacuum. Experiment shows that, besides absorption and stimulated emission of a quantum $\hbar\omega_\mathbf{q}$, spontaneous emission may happen in an electromagnetic vacuum. In Einstein's 1916 theory this was accounted for phenomenologically. It is justified quantum-theoretically by quantizing each mode $\mathbf{q}$ of the electromagnetic field, as displayed in Table 2. Then, the rate of emission of a light quantum by the atom is proportional to $n_\mathbf{q} + 1$, while the rate of absorption of a quantum is proportional to $n_\mathbf{q}$, where $n_\mathbf{q}$ is the occupancy (number of photons) of mode $\mathbf{q}$.

Table 2. A classical electromagnetic field is a weighted sum of plane-wave terms, $\widetilde{A}_\mathbf{q} \exp[+\mathrm{i}(\mathbf{q}\cdot\mathbf{r} - \omega_\mathbf{q} t)] + \widetilde{A}_\mathbf{q}^* \exp[-\mathrm{i}(\mathbf{q}\cdot\mathbf{r} - \omega_\mathbf{q} t)]$, where $\widetilde{A}_\mathbf{q}$ is a dimensionless field amplitude. For each $\mathbf{q}$ there exist two orthogonal polarizations, not shown in the table.

Classical electrodynamics	Quantum electrodynamics
scalar $\widetilde{A}_\mathbf{q} \exp(-\mathrm{i}\omega_\mathbf{q} t)$	annihilation *operator* $a_\mathbf{q}$ for photon absorption
scalar $\widetilde{A}_\mathbf{q}^* \exp(+\mathrm{i}\omega_\mathbf{q} t)$	creation *operator* $a_\mathbf{q}^\dagger$ for photon emission
$[\widetilde{A}_\mathbf{q}, \widetilde{A}_\mathbf{q}^*] = 0$	$[a_\mathbf{q}, a_\mathbf{q}^\dagger] = 1$

If the field is in thermal equilibrium at temperature T, then $n_\mathbf{q}$ is a random variable having a multiplicity of realisations. It is ruled by the Planck–Bose statistics; the mean $\langle n_\mathbf{q}\rangle$ is such that

$$\frac{\langle n_\mathbf{q}\rangle}{\langle n_\mathbf{q}\rangle + 1} = \exp\left(-\frac{\hbar\omega_\mathbf{q}}{kT}\right), \tag{17}$$

and the variance is $\langle n_\mathbf{q}\rangle(1 + \langle n_\mathbf{q}\rangle)$. An ensemble of atoms coupled to that thermal field eventually gets equilibrated at the field's temperature [1].

Similarly the thermal equilibration of a guest electron by the host crystal at a well-defined temperature is only possible if the elastic deformation field is quantized [14]. In the following calculations, *quantum* elastodynamics will be approximated by *stochastic* elastodynamics such that the dimensionless amplitude $\widetilde{A}_\mathbf{q}$ is taken as a stochastic scalar, instead of an operator, whose phase is equally distributed between $-\pi$ and $+\pi$, and whose squared modulus $|\widetilde{A}_\mathbf{q}|^2$ is $n_\mathbf{q} + ½$, where $n_\mathbf{q}$ is the random number of phonons in mode $\mathbf{q}$ as ruled by the Planck–Bose statistics.

6 Disorder correction to thermodynamic equilibrium

This section specializes the previous findings to the case of thermodynamic equilibrium. Then, several terms in the kinetic equation (14) vanish,

$$\frac{\partial f_0}{\partial t} = 0, \tag{18}$$

$$W_{\mathbf{p}',\mathbf{p}} f_0(\mathbf{p}',\mathbf{r})[1-f_0(\mathbf{p},\mathbf{r})] - W_{\mathbf{p},\mathbf{p}'} f_0(\mathbf{p},\mathbf{r})[1-f_0(\mathbf{p}',\mathbf{r})] = 0, \tag{19}$$

$$\left(\frac{\partial E}{\partial \mathbf{p}}\right)\cdot\frac{\partial f_0}{\partial \mathbf{r}} + \left(-\frac{\partial U_1}{\partial \mathbf{r}}\right)\cdot\frac{\partial f_0}{\partial \mathbf{p}} = 0. \tag{20}$$

The middle line above expresses detailed balance in scattering events [14, 41]. The last line is a consequence of the first two. The solution is

$$f_0(\mathbf{r},\mathbf{p}) = f_{\mathrm{FD}}\left(\frac{E(\mathbf{p}) - g(\mathbf{r})}{kT}\right) \equiv f_\mathrm{e}(\mathbf{r}, E(\mathbf{p})), \tag{21}$$

where $f_{\mathrm{FD}}(y) \equiv (\mathrm{e}^y + 1)^{-1}$ is the Fermi–Dirac function, and $g(\mathbf{r}) = \tilde{g} - U_1(\mathbf{r})$ is the chemical potential of the electron gas whose electrochemical potential $\tilde{g}$ is independent of position in a state of equilibrium.

We are henceforth interested in the first stochastic correction to f_0, as given in section 4 by

$$f_1(\mathbf{r},\mathbf{r}',\mathbf{p},t) = \left(\frac{\partial f_\mathrm{e}}{\partial E}\right)_\mathbf{r} u(\mathbf{r}',t). \tag{22}$$

The covariance of the Wigner function $f_\mathrm{W} \approx f_0 + f_1$ is

$$C_\mathrm{W}(\mathbf{s}) \equiv \langle f_1(\mathbf{r},\mathbf{r}'+\mathbf{s},\mathbf{p},t) f_1(\mathbf{r},\mathbf{r}',\mathbf{p},t)\rangle = \left(\frac{\partial f_\mathrm{e}}{\partial E}\right)_\mathbf{r}^2 C_U(\mathbf{s}). \tag{23}$$

The Wigner function has thus the same correlation length as the energyscape. Figure 4 below shows that

(i) in an almost filled ($g - E \gg kT$) or almost empty ($E - g \gg kT$) Bloch state, the Wigner function is an almost deterministic quantity equal to 1 or 0;

(ii) at the Fermi level $E = g$, the Wigner function is a stochastic quantity of mean ½ and variance

$$\Delta f_\mathrm{W}^2 \equiv C_\mathrm{W}(s=0)\big|_{E=g} = \left(\frac{u_0}{4kT}\right)^2. \tag{24}$$

Figure 4 below, just like Fig. 3 above, shows *one* realisation of the Wigner function together with the mean function. The latter is restricted to the range 0–1 as it is the occupation *probability* of a fermion state, while the former may lie outside this range as it is a *quasi*-probability. In the next section the present results are specialized to GaAs with the physical parameters of section 2.

[1] Just like a boson (here, a photon) gas in an equilibrium state can thermalise a fermion (here, an electron) gas through boson-fermion scattering events, conversely a fermion gas in equilibrium can thermalise a boson gas [39, 40]. Thermalisation is only possible if spontaneous boson emission, not accountable for in terms of classical fluctuations of the boson field, is included.

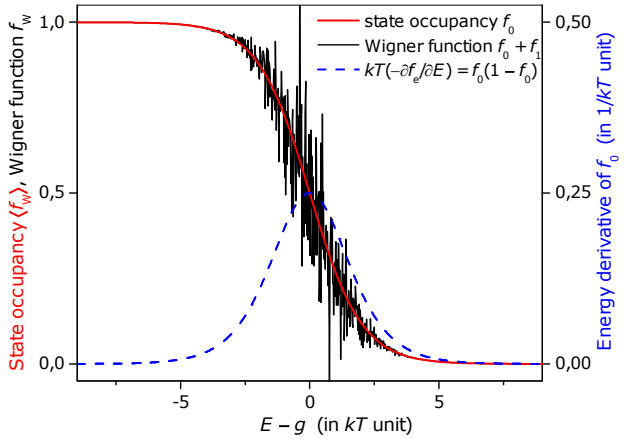

Fig. 4. State occupancy in thermodynamic equilibrium $\langle f_W \rangle = f_0$, energy derivative thereof, and Wigner function $f_W \approx f_0 + f_1$ are plotted against energy E varying around the chemical potential $g(\mathbf{r})$ of the electron gas.

7 Application to a perfect GaAs wire

7.1 The electron-lattice interaction

In GaAs a conduction electron of energy lying within a range $\approx kT$ about the Fermi level as shown in Fig. 2 only couples to acoustic vibrations. The coupling can occur in two ways, via a macro- or a microscopic field, as displayed in Table 3. In polar GaAs, an electron senses the macroscopic electric field due to the polarization generated by the differential displacement of the cationic (Ga) and anionic (As) sublattices. Another coupling of a non-polar kind exists in any crystal, whether ionic or covalent. It arises from the dependence of the electronic energy band on the deformation (strain) associated with an acoustic wave [20, 42–44].

Table 3. The two kinds of electron-phonon coupling in a polar material.

Polar interaction	Non-polar interaction
***macro*field**	***micro*field**
‘ piezoelectric ’ (pz)	‘ deformation potential ’ (dp)

The polar interaction is akin to the interaction of an electron with an electric field in vacuum, as displayed in Table 4, where ε henceforth denotes the static permittivity of the solid medium, and K_{pz} is the electro-mechanical coupling coefficient such that K_{pz}^2 is the ratio of the electrical energy in the piezoelectric field generated by the acoustic wave to the total (electrical + mechanical) energy [20, 43, 44].

Table 4. Electron-phonon interaction mediated by a macroscopic electric field in a polar material compared to electron-photon interaction in a vacuum.

Electrodynamics	Elastodynamics
electron-***photon*** coupling constant $\alpha = \dfrac{e^2}{4\pi\varepsilon_0\hbar c}$	electron-***phonon*** coupling constant $\alpha_{pz} \equiv \dfrac{(K_{pz}e)^2}{4\pi\varepsilon\hbar c_s}$

The polar electron-lattice interaction energy may be written [45]

$$U_{pz}(\mathbf{r},t) = \hbar c_s \left(\frac{2\pi\alpha_{pz}}{\Omega}\right)^{1/2} \sum_{\mathbf{q}} \frac{1}{\sqrt{q}} \left[\tilde{A}_{\mathbf{q}}\, e^{+i(\mathbf{q}.\mathbf{r} - \omega_q t)} + \tilde{A}_{\mathbf{q}}^{\,*}\, e^{-i(\mathbf{q}.\mathbf{r} - \omega_q t)}\right]. \quad (25)$$

The interaction energy has been simplified in two ways. First, the actual energy depends on the acoustic wave's polarisation which can be longitudinal or transverse. In (25) averaging over polarisations has been carried out. Secondly, the actual energy depends on the direction of the wave-vector $\mathbf{q}$ via K_{pz}^2. In (25) a directional average $(K_{pz}^2)_{av}$ has been taken so that an isotropic description results; see details in [20].

The non-polar electron-lattice interaction energy $U_{dp}(\mathbf{r},t)$ is $\Xi \operatorname{div} \mathbf{a}(\mathbf{r},t)$, where $\operatorname{div} \mathbf{a}(\mathbf{r},t)$ is the dilatation of the lattice due to the acoustic wave, and the deformation-potential constant Ξ is the shift of the conduction-band bottom per unit dilatation [14, 20, 42]. In a simplified isotropic description,

$$U_{dp}(\mathbf{r},t) = \frac{\hbar^2}{m^*} \left(\frac{\alpha_{dp}}{\Omega}\right)^{1/2} \sum_{\mathbf{q}} i\sqrt{q} \left[\tilde{A}_{\mathbf{q}}\, e^{+i(\mathbf{q}.\mathbf{r} - \omega_q t)} - \tilde{A}_{\mathbf{q}}^{\,*}\, e^{-i(\mathbf{q}.\mathbf{r} - \omega_q t)}\right], \quad (26)$$

where

$$\alpha_{dp} \equiv \frac{(m^*\Xi)^2}{2\hbar^3 \rho c_s} \quad (27)$$

is a dimensionless coupling constant, and ρ is the mass density.

Table 5. Physical quantities of GaAs used in the paper; ρ, M, c_s, K_{pz}^2, ε and Ξ are taken from Ridley's textbook [20]; q_D and q_{TF}^{-1} are computed from (31) and (33).

Quantity	Notation	Value
Mass density	ρ	5.32×10^3 kg/m^3
Mass of GaAs	M	2.4×10^{-25} kg
Speed of sound	c_s	4.0×10^3 m/s
Squared electromechanical constant	$(K_{pz}^2)_{av}$	0.00252
Static permittivity	ε	$13.2\,\varepsilon_0$
Deformation-potential constant	Ξ	+7.0 eV
Debye wave-vector	q_D	1.1×10^{10} m^{-1}
Thomas–Fermi screening length	q_{TF}^{-1}	0.8×10^{-9} m

Table 5 above lists the numerical values of the physical quantities involved. From the table we compute $\alpha_{dp} \approx 10^{-4}$ and $\alpha_{pz} = 10^{-1}$ in GaAs. This suggests that the piezoelectric interaction dominates when coupling is with the acoustic vibrations. On adopting different definitions of the coupling constants (see appendix A), this is also the conclusion reached by Ridley [20]. Likewise, Balkanski and Wallis state that ‘ in lightly doped n-GaAs and n-InSb, piezoelectric scattering dominates the scattering of thermal electrons at low temperatures ’ [44]. Davies, however, remarks that ‘ there remains considerable dispute over the relative importance of deformation-potential and piezoelectric

coupling in GaAs' [46]. Since opinions about the subject-matter are divided, both electron-phonon interactions will be addressed in the next subsection.

7.2 The disorder correction in GaAs

For a piezoelectric interaction as described by (25), the covariance of the random potential energy buffeting the mobile electrons is given by

$$C_U(\mathbf{s}) = u_0^2 \widetilde{C}(\tilde{s}), \tag{28}$$

$$u_0^2 = \frac{2\alpha_{pz}}{\pi} kT\hbar\omega_D, \tag{29}$$

$$\widetilde{C}(\tilde{s}) = \frac{1}{\tilde{s}} \int_0^{\tilde{s}} \frac{\sin u}{u} \mathrm{d}u, \tag{30}$$

where $\omega_D \equiv c_s q_D$ is the Debye cut-off frequency,

$$q_D \equiv \left(6\pi^2 \frac{\rho}{M}\right)^{1/3} \tag{31}$$

is the Debye wave-vector, M is the mass of GaAs, and lastly $\tilde{s} \equiv q_D s$ is the separation distance reckoned in units of $1/q_D$. The normalized covariance $\widetilde{C}(\tilde{s})$ is shown in Fig. 5 below.

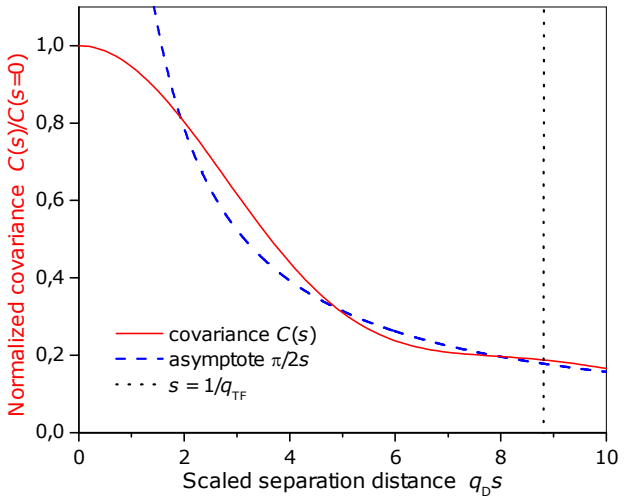

Fig. 5. Normalized covariance of the unscreened piezoelectric electron-phonon interaction, plotted against the scaled separation distance. The scaled Thomas–Fermi screening length in the GaAs example is marked as a vertical dotted line.

The correlation length, defined as

$$l_c \equiv \int_0^{+\infty} \widetilde{C}(s)\,\mathrm{d}s, \tag{32}$$

diverges logarithmically as $\tilde{s}\,\widetilde{C}(\tilde{s})|_{\tilde{s}\gg 1}$ is the Dirichlet integral $\pi/2$. The divergence is due to the infinite range of the Coulomb potential if screening by mobile charges is not accounted for when calculating the macroscopic electric field of bound charges. Including screening entails an extra factor $q^4/(q^2+q_{TF}^2)^2$ [20], where

$$q_{TF} \equiv \left[\frac{(2m^*)^{3/2} e^2 E_F^{1/2}}{2\pi^2\hbar^3\varepsilon}\right]^{1/2} \tag{33}$$

is the reciprocal Thomas–Fermi length. The normalized covariance takes on the form

$$\widetilde{C}(s) = \int_0^{q_D} \frac{q^4}{(q^2+q_{TF}^2)^2} \frac{\sin(qs)}{qs} \mathrm{d}q, \tag{34}$$

wherefore the correlation length (32) is

$$l_c = \frac{\pi}{4q_{TF}} \left\{ \ln\left[1+\left(\frac{q_D}{q_{TF}}\right)^2\right] + \left[1+\left(\frac{q_D}{q_{TF}}\right)^2\right]^{-1} - 1 \right\}. \tag{35}$$

In the GaAs example, l_c = 2.1 nm. The fluctuations in the random potential energy and the Fermi-level occupancy are given in Table 6 below.

Table 6. Unscreened piezoelectric electron-phonon coupling in GaAs. Root-mean-square (r.m.s.) fluctuation in the interaction energy and ensuing r.m.s. fluctuation in the Wigner function at the Fermi level. Numerical values are computed at T = 4 K.

Absolute fluctuation in U_2	$u_0 = \left(\frac{2\alpha_{pz}}{\pi} kT\hbar\omega_D\right)^{1/2}$ $= 0.81\times10^{-3}$ eV
Relative fluctuation in U_2	$\frac{u_0}{kT} = \left(\frac{2\alpha_{pz}}{\pi}\frac{\hbar\omega_D}{kT}\right)^{1/2}$ $= 2.35$
Fluctuation in f_W at Fermi level	$\Delta f_W = \frac{u_0}{4kT} = 0.59$

For a deformation-potential interaction as described by (26), the covariance of the random potential energy buffeting the mobile electrons is such that [14]

$$u_0^2 = \frac{kT\Xi^2}{2Mc_s^2}, \tag{36}$$

$$\widetilde{C}(\tilde{s}) = 3\frac{\sin\tilde{s} - \tilde{s}\cos\tilde{s}}{\tilde{s}^3}, \tag{37}$$

$$l_c = \frac{3\pi}{4q_D}. \tag{38}$$

In the GaAs example, l_c = 0.21 nm. The fluctuations in the random potential energy and in the Fermi-level occupancy are given in Table 7 below.

Table 7. Deformation-potential electron-phonon coupling in GaAs. Root-mean-square (r.m.s.) fluctuation in the interaction energy and ensuing r.m.s. fluctuation in the Wigner function at the Fermi level. Numerical values are computed at T = 4 K.

Absolute fluctuation in U_2	$u_0 = \left(\frac{kT}{Mc_s^2}\right)^{1/2}\lvert\Xi\rvert$ $= 2.6\times10^{-2}$ eV
Relative fluctuation in U_2	$\frac{u_0}{kT} = \frac{\lvert\Xi\rvert}{(kTMc_s^2)^{1/2}}$ $= 76$
Fluctuation in f_W at Fermi level	$\Delta f_W = \frac{u_0}{4kT} = 19$

To conclude this section, for both electron-phonon interactions the fluctuation of the Wigner function due to the stochastic nature of thermal agitation is significant

about the Fermi level. The Wigner function will leave the range 0–1 for some realisations of the lattice agitation. Our calculations show that the non-polar interaction is more effective in this respect than the polar one. At this stage a word of caution is necessary. For the perturbation expansion (13) of the Wigner function to be accurate at the Fermi level, $\langle f_1^2\rangle/f_0^2 = (u_0/kT)^2$ should be less than unity. As $u_0 \propto T^{1/2}$, the expansion is quantitatively valid at high temperatures. For the polar (non-polar) interaction, this means $T > \alpha_{pz}\hbar\omega_D/2\pi k = 5$ K ($T > \Xi^2/8Mc_s^2k = 300$ K). At lower temperatures, the large relative fluctuation of f_W is unlikely to be given by the perturbative result $u_0/4kT$.

8 Conclusions

The present study was motivated by the issue of a quantum-mechanically coherent motion of electrons over a significant distance in a solid wire. Such a motion is expected in a semiconductor structure where electron scattering by structural defects and impurities is avoided, and scattering by lattice vibrations is minimized by lowering the temperature. A large electronic mean free path is achieved, and in addition the infrequent scattering events are almost elastic. This makes the internal wire resistance vanish [24]. Classically speaking the lattice is almost frozen, and one expects electron motion to be hardly affected by the thermal disorder of the lattice. To check this, we have determined the electronic Wigner function —which supersedes the phase-space occupation function of classical physics— for realistic values of the physical parameters (electron density, electron-phonon coupling ...) taken from a specific experimental system. We have found that the thermal disorder of the lattice significantly affects the Wigner function of the electrons whose energies lie about the Fermi level and which carry the current.

Both the polar and non-polar interactions of electrons with the disordered lattice have been examined. Below 100 K the polar interaction limits the mobility of GaAs electrons more effectively than the non-polar interaction, as seen in Fig. 7 of [19]; that is, the polar interaction is more effective than the non-polar one as far as mobility is concerned. This holds in intrinsic GaAs while in the degenerate GaAs considered herein, the polar interaction is weakened by electrical screening; see appendix B where the theoretical mean free path due to either a polar or a non-polar interaction with phonons is compared to the experimental value measured in the quasi-2D gas. As far as the fluctuation of the Wigner function at the Fermi level is concerned, it is not affected by the interaction in the same way as the mobility owing to the different dependencies on the physical parameters. The fluctuation is rewritten here, in the high-temperature range, as

$$\Delta f_W\big|_{dp} = \frac{1}{m^*}\left(\frac{\hbar^3\rho\,\alpha_{dp}}{8Mc_skT}\right)^{1/2}, \qquad (39)$$

$$\Delta f_W\big|_{pz} = \left(\frac{\hbar\omega_D\alpha_{pz}}{8\pi kT}\right)^{1/2}. \qquad (40)$$

The different patterns of (39) and (40) explain why the fluctuation of the Wigner function is larger for the non-polar interaction in spite of its smaller coupling constant.

Qualitatively speaking, the fluctuation of the Wigner function about its equilibrium value is expected to be important when the lattice is almost frozen at $T = 4$ K. Then, insofar as a physical quantity is reliant upon the actual realisation of the disordered energyscape, the perfect electric wire is likely to show irreproducible behaviour, even if no electric current is flowing. The lattice, however, is not really frozen at 4 K since the mean number of acoustic phonons is significant, $\langle n_{\mathbf{q}}\rangle \approx 62$, at the typical wave-vector involved in electron-phonon scattering. A change in the behaviour of the Wigner-function fluctuation is expected in the zero-point regime such that the mean number of acoustic phonons is less than unity and the agitation becomes independent of temperature. This happens at temperatures significantly lower than $m^*c_s^2/k = 0.065$ K in GaAs, i.e. five times lower than the temperature achieved in the experiment.

I am indebted to Jean-Claude Serge Lévy (Université de Paris Cité) for inviting me to participate in the Tenth Complexity–Disorder Days (27–28 January 2025), and to Henri Bringuier for the numerical determination of the covariance of the unscreened piezoelectric interaction..

Appendix A. Alternative definition of the electron-phonon coupling constant

In section 6 a dimensionless electron-phonon coupling constant of the piezoelectric interaction was defined in analogy with quantum electrodynamics in Table 4. A coupling constant (27) of the deformation-potential interaction is defined so as to provide a simple formula (26) for the interaction Hamiltonian. Now Ridley defines a coupling constant α_{ep} in the same way for both interactions following general quantum field theory, i.e. considering that a conduction electron dressed by virtual phonons has its effective mass renormalized, $m^* \to m^{**}$, according to [20]

$$\frac{1}{m^{**}} = \frac{1}{m^*}\left(1 - \frac{\alpha_{ep}}{6}\right). \qquad (A.1)$$

This approach is reminiscent of Fröhlich's polaron theory where an electron interacting with the optical vibrations of an ionic lattice has its inertia increased by a cloud of virtual optical phonons. From his calculation of m^{**}, Ridley obtains the coupling strengths

$$\alpha_{ep}\big|_{pz} = \frac{(K_{pz}e)^2}{\pi^2\varepsilon\hbar c_s}, \qquad (A.2)$$

$$\alpha_{ep}\big|_{dp} = \frac{8(m^*\Xi)^2}{\pi^2\hbar^3\rho c_s}\ln\left(\frac{\hbar q_D}{2m^*c_s}\right) \qquad (A.3)$$

Our and Ridley's expressions of the piezoelectric coupling strength differ in a factor

$$\frac{\alpha_{ep}\big|_{pz}}{\alpha_{pz}} = \frac{4}{\pi}, \qquad (A.4)$$

which is very close to unity. Our and Ridley's expressions of the deformation-potential coupling strength differ in a factor

$$\frac{\alpha_{ep|_{dp}}}{\alpha_{dp}} = \left(\frac{4}{\pi}\right)^2 \ln\left(\frac{\hbar q_D}{2m^* c_s}\right), \qquad \text{(A.5)}$$

whose numerical value 12.6 is significantly greater than unity. So our $\alpha_{dp} \approx 10^{-4}$ would misestimate the coupling compared to Ridley's $\alpha_{ep|_{dp}} \approx 1.2\text{x}10^{-3}$. Since we have found in section 7 that the fluctuation caused by the polar interaction is smaller than the one caused by the non-polar interaction in GaAs, we conclude that coupling strengths do not correctly reflect the relative effect of both interactions on Wigner-function fluctuations, while they are relevant as far as renormalization of the effective mass is concerned.

Appendix B. Theoretical electron-phonon mean free path

In section 3 a value $\lambda = v_F m^* \mu = 33$ μm of the mean free path was inferred from the measured mobility $e\mu$ of the quasi-2D electron gas and the Fermi velocity v_F in GaAs at 0.3 K. This large value of λ was tentatively ascribed to one single limiting scattering mechanism, namely with acoustic phonons. Now the theoretical formulae in a 3D electron gas, respectively for the non-polar and the polar interaction, are (3.79) and (3.180) in [20], namely

$$\lambda_{dp} = \pi \left(\frac{\hbar^2}{m^* \Xi}\right)^2 \frac{\rho c_s^2}{kT}, \qquad \text{(B.1)}$$

$$\lambda_{pz} = v_F \tau_v(E_F)|_{pz}, \qquad \text{(B.2)}$$

where

$$\frac{1}{\tau_v(E_F)}\bigg|_{pz} = \alpha_{pz} \frac{kT}{\hbar} \frac{2c_s}{v_F} \left[1 + \frac{1}{1+\eta} - \frac{2}{\eta} \ln(1+\eta)\right], \qquad \text{(B.3)}$$

and

$$\eta \equiv \frac{8m^* E_F}{(\hbar q_{TF})^2} \qquad \text{(B.4)}$$

is a dimensionless parameter which vanishes for strong screening. In this limit (B.3) shows that α_{pz} is renormalized into $\eta^2 \alpha_{pz}/3$, and $\eta = 7.5\text{x}10^{-3}$. The ensuing rate of velocity relaxation is calculated to be very small, $1/\tau_v(E_F)|_{pz} = 10^6\ \text{s}^{-1}$, and the mean free path, $\lambda_{pz} = 0.2$ m, is very large. Thereby the piezoelectric electron-phonon interaction is so strongly screened in the degenerate electron gas that it plays no role in limiting the free path. In contrast, the deformation-potential interaction entails a mean free path $\lambda_{dp} = 1.7\text{x}10^{-3}$ m at $T = 0.3$ K, closer to the experimental one, $\lambda = 33$ μm. The fact that the theoretical mean free path overestimates the experimental one cannot be ascribed to the geometry of the quasi-2D gas. The overestimation stems from the neglect of an extra scattering mechanism with residual, unintentional neutral impurities, not accounted for in the present paper, lowering the mobility in the actual material. Figure 7 of [19] shows a limiting value $e\mu \approx 3\text{x}10^6\ \text{cm}^2\text{V}^{-1}\text{s}^{-1}$ below 8 K due to neutral impurities.

References

1. M. Mitchell Waldrop, Quantum computing, *Technology Review* (M.I.T.) **103**, 60–66 (2000)
   M. Mitchell Waldrop, L'ordinateur quantique, un rêve qui devient réalité, *Courrier international* **498**, 58–59 (2000) (French translation)
2. X. Waintal, The quantum house of cards, *Proc. Nat. Acad. Sci. USA* **121**, e2313269120 (2024)
3. M. Schlosshauer, Quantum decoherence, *Phys. Reports* **831**, 1–57 (2019)
4. E. Bringuier, The basis of the semiclassical description of electron transport in solids, *Eur. J. Phys.* **42**, 025502 (2021)
5. E. Bringuier, Disorder-induced quantum-to-classical transition, or how the world becomes classical, *Eur. Phys. J. Web Conf.* **263**, 01011 (2022)
6. E. Verdet, *Leçons d'Optique physique I* (Imprimerie Impériale, Paris, 1869) section 75
7. Lord Rayleigh, On the resultant of a large number of vibrations of the same pitch and of arbitrary phase, *Phil. Mag.* **10**, 73–78 (1880)
8. P. Debye and A. M. Bueche, Scattering by an inhomogeneous solid, *J. Appl. Phys.* **20**, 518–525 (1949)
9. R. Landauer, Can a length of perfect conductor have a resistance ?, *Phys. Lett.* **85A**, 91–93 (1981)
10. L. Pfeiffer, A. Yacoby, H. L. Stormer, K. L. Baldwin, J. Hasen, A. Pinczuk *et al.*, Transport and optics in quantum wires fabricated by MBE overgrowth on the (110) cleaved edge, *Microelectronics Journal* **28**, 817–823 (1997)
11. R. de Picciotto, H. L. Stormer, L. N. Pfeiffer, K. W. Baldwin and K. W. West, Four-terminal resistance of a ballistic quantum wire, *Nature* **411**, 51–54 (2001)
12. E. Bringuier, La résistance électrique abolie, *La Recherche* **345**, 22–23 (2001)
    E. Bringuier, La resistencia eléctrica, abolida, *Mundo científico* **228**, 14–15 (2001) (Spanish translation)
13. J. Bardeen, Conduction : metals and semiconductors, *Handbook of Physics* 2nd edn, edited by E. U. Condon and H. Odishaw (McGraw-Hill, New York, 1967) pp 4-72–4-101
14. E. Bringuier, Order to disorder transformation in an Ohmic resistor : Quantum theory of Joule heating, *Eur. Phys. J. Web Conf.* **300**, 01010 (2024)
15. C. Henkel, Coherent transport, *C. R. Acad. Sci.* (Paris) **2**, 573–580 (2001)
16. L. Ryzhik, G. Papanicolaou and J. B. Keller, Transport equations for elastic and other waves in random media, *Wave Motion* **24**, 327–370 (1996)
17. E. P. Wigner, Quantum-mechanical distribution functions revisited, *Perspectives in Quantum Theory : Essays in Honor of Alfred Landé,* edited by W. Yourgrau and A. van der Merwe (The MIT Press, Cambridge, MA, 1971, and Dover, New York, 1979) pp. 25–36
18. C. Weisbuch, Fundamental properties of III–V semiconductor two-dimensional quantized structures : The basis for optical and electronic device

applications, *Applications of multiquantum wells, selective doping, and superlattices*, Semiconductors and Semimetals vol. **24**, edited by R. Dingle (Academic, San Diego, CA, 1987) pp. 1–133
19. G. E. Stillman and C. M. Wolfe, Electrical characterization of epitaxial layers, *Thin Solid Films* **31**, 69–88 (1976)
20. B. K. Ridley, *Quantum Processes in Semiconductors* 4th edn (Clarendon, Oxford, 1999) chapter 3
21. B. J. van Wees, H. van Houten, C. W. J. Beenakker, J. G. Williamson, L. P. Kouwenhoven, D. van der Marel *et al.*, Quantized conductance of point contacts in a two-dimensional electron gas, *Phys. Rev. Lett.* **60**, 848–850 (1988)
22. D. A. Wharam, T. J. Thornton, R. Newbury, M., Pepper, H. Ahmed, J. E. F. Frost *et al.*, One-dimensional transport and the quantisation of the ballistic resistance, *J. Phys. C: Solid State Physics* **21**, L209–L214 (1988)
23. R. Landauer, Conductance determined by transmission: probes and quantised constriction resistance, *J. Phys.: Condens. Matter* **1**, 8099–8110 (1989)
24. E. Bringuier, Ohm's law of electrical conduction at the nanoscale, *2D and 3D Nanostructures: Structures, Properties and Applications*, edited by J.-C. S. Lévy (Jenny Stanford, Singapore, 2026) pp. 21–46
25. F. B. Pedersen, Simple derivation of the effective-mass equation using a multiple-scale technique, *Eur. J. Phys.* **18,** 43–45 (1997)
26. M. Casas, H. Krivine and J. Martorell, On the Wigner transforms of some simple systems and their semiclassical interpretation, *Eur. J. Phys.* **12**, 105–111 (1991)
27. J. M. Sellier and I. Dimov, On the simulation of indistinguishable fermions in the many-body Wigner formalism, *J. Comput. Phys.* **280**, 287–294 (2015)
28. E. Garber, S. G. Brush and C. W. F. Everitt (editors), *Maxwell on Heat and Statistical Mechanics: On ''Avoiding All Personal Enquiries'' of Molecules* (Lehigh University Press, Bethlehem, PA, 1995) p. 422
29. M. D. Sturge, *Statistical and Thermal Physics* (A. K. Peters, Natick, MA, 2003) p. 39
30. P. W. Anderson, Absence of diffusion in certain random lattices, *Phys. Rev.* **109**, 1492–1505 (1958)
31. A. H. Nayfeh, *Perturbation Methods* (Wiley, New York, 1973) chapter 6
32. N. G. van Kampen, Elimination of fast variables, *Phys. Reports* **124**, 69–160 (1985)
33. E. Vanmarcke, *Random Fields* (The MIT Press, Cambridge, MA, 1983) p. 31
34. J. M. Ziman, *Models of Disorder: The theoretical physics of homogeneously disordered systems* (Cambridge University Press, Cambridge, 1979) chapter 3
35. P. M. Richards, Evolution of energy distribution in a model system without conventional Lorentzian lifetime broadening, *Phys. Rev. B* **60**, 4778–4783 (1999)
36. L. A. Bányai, *Lectures on Non-Equilibrium Theory of Condensed Matter* (World Scientific, Singapore, 2006) chapter 5
37. J. M. Ziman, *Elements of Advanced Quantum Theory* (Cambridge University Press, Cambridge, 1969) section 2.4
38. L. W. Nordheim, On the kinetic method in the new statistics and its application in the electron theory of conductivity, *Proc. Roy. Soc. London* A **CXIX**, 689–698 (1928)
39. A. S. Kompaneets, The establishment of thermal equilibrium between quanta and electrons, *Zh. Eksp. Teor. Fiz.* **31**, 876–885 (1956)
Sov. Phys. JETP **4**, 730–737 (1957) (English translation)
40. G. E. Freire Oliveira, C. Maes and K. Meerts, On the derivation of the Kompaneets equation, *Astropart. Phys.* **133**, 102644 (2021)
41. C. Kittel, *Elementary Statistical Physics* (Dover, Mineola, NY, 2004) chapters 36 and 37
42. J. Bardeen and W. Shockley, Deformation potentials and mobilities in non-polar crystals, *Phys. Rev.* **80**, 72–80 (1950)
43. L. M. Roth, Dynamics and classical transport of carriers in semiconductors, *Handbook on Semiconductors*, vol. **1** edited by P. T. Landsberg (Elsevier, Amsterdam, 1992) chapter 10
44. M. Balkanski and R. F. Wallis, *Semiconductor Physics and Applications* (Oxford University Press, New York, 2000) section 8.5
45. G. Whitfield, J. Gerstner and K. Tharmalingam, Motion of the piezoelectric polaron at zero temperature, *Phys. Rev.* **165**, 993–998 (1968)
46. J. H. Davies, *The Physics of Low-Dimensional Semiconductors* (Cambridge University Press, Cambridge, 1998) p. 305